

Electron Transport in a Multi-Channel One-Dimensional Conductor: Molybdenum Selenide Nanowires

Latha Venkataraman, Yeon Suk Hong, and Philip Kim
Department of Physics, Columbia University, New York, New York 10027
(Dated: September 13, 2018)

We have measured electron transport in small bundles of identical conducting Molybdenum Selenide nanowires where the number of weakly interacting one-dimensional chains ranges from 1-300. The linear conductance and current in these nanowires exhibit a power-law dependence on temperature and bias voltage respectively. The exponents governing these power laws decrease as the number of conducting channels increase. These exponents can be related to the electron-electron interaction parameter for transport in multi-channel 1-D systems with a few defects.

PACS numbers: 72.15.Nj,73.23.Hk,73.90.f

Interacting electrons in one-dimensional (1D) metals constitute a Luttinger Liquid (LL)[1], in contrast to a Fermi liquid (FL) in 3-dimensional (3D) metals. Transport properties of 1D conductors are strongly modified as adding an electron to a 1D metal requires changing the many-body state of its collective excitations. This results in vanishing electron tunneling density of states at low energy. Power-law dependent suppression in tunneling conductance has been observed in many systems, including fractional quantum Hall edge states [2], single and multi-walled carbon nanotubes [3, 4, 5], bundles of NbSe_3 nanowires [6] and conducting polymers [7]. A cross-over from a truly 1D Luttinger-liquid (LL) to a 3D Fermi-liquid (FL) is expected as 1D conductors are coupled together, increasing the number of weakly interacting channels [8, 9]. This transition, however, has not been observed in the above (quasi) 1-D systems due to the experimental difficulty in preparing identical conducting quantum wires to form conductors with a few weakly interacting channels. In this letter, we report temperature and bias dependent electric transport measurements on small bundles of Molybdenum Selenide (MoSe) nanowires [10, 11, 12], whose diameter ranges from 1-15 nm. These nanowires, which consist of bundles of weakly interacting and electrically identical 1D MoSe molecular chains, show a power-law dependent tunneling conductance. The exponent governing the power-law decreases as the bundle diameter increases, indicating a transition from 1D to bulk transport with increasing number of conducting channels.

Crystalline bundles of MoSe chains are obtained from the dissolution of quasi-1D $\text{Li}_2\text{Mo}_6\text{Se}_6$ crystals in polar solvents. Single crystal $\text{Li}_2\text{Mo}_6\text{Se}_6$ was prepared as described previously [13]. X-ray diffraction analysis showed hexagonally close packed molecular MoSe chains with a lattice spacing $a_0 = 0.85$ nm, separated by Li atoms (Fig. 1(a)). Atomic scale bundles of MoSe nanowires were produced from $\sim 100 \mu\text{M}$ solutions of $\text{Li}_2\text{Mo}_6\text{Se}_6$ in anhydrous methanol. The solutions were then spun onto degenerately doped Si/SiO₂ substrates with lithographically patterned electrodes in a Nitrogen atmosphere.

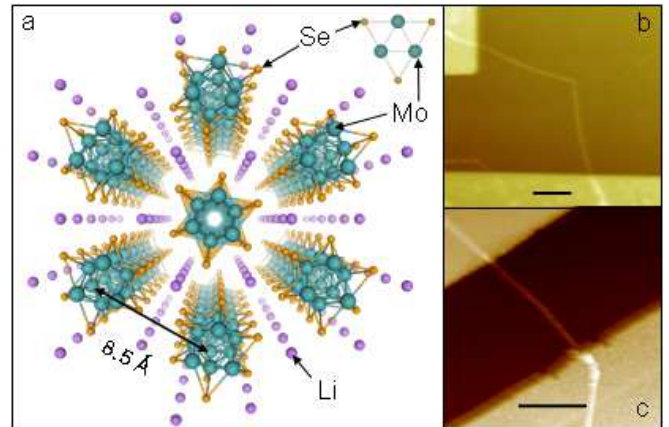


FIG. 1: (color online) (a) Structural model of a 7-chain MoSe nanowire along with the triangular Mo_3Se_3 unit cell, (b) and (c) AFM height images of MoSe nanowires between two Au electrodes. The wire heights are 7.2 nm and 12.0 nm respectively. Scale bar = 500 nm.

Typically, 35 nm thick Au electrodes with 5 nm Cr adhesion layer separated by $\sim 1 \mu\text{m}$ were used to contact randomly deposited nanowires. Figs. 1(b) and (c) show atomic force microscope (AFM) images of typical devices. The two-probe resistance of such a device, which ranged from $\sim 100 \text{ k}\Omega$ – $100 \text{ M}\Omega$ at room temperature, was measured in a cryostat with a continuous flow of helium. A degenerately doped silicon substrate, underneath a $L_{ox} = 300$ nm thick silicon dioxide dielectric layer, served as a back gate to modulate the charge density in the nanowires. Once transport measurements were complete, the wire diameter, D , was determined from an AFM height profile.

Fig. 2 shows the conductance (G) normalized by its room temperature value as a function of temperature (T) for a representative subset of the samples studied [20]. We applied a small bias voltage, ($V \ll k_B T/e$), to stay in the linear response regime for this measurement. Notably, the mesoscopic scale samples ($D < 20$ nm, $L \sim 1 \mu\text{m}$) exhibit more than two orders of magnitude

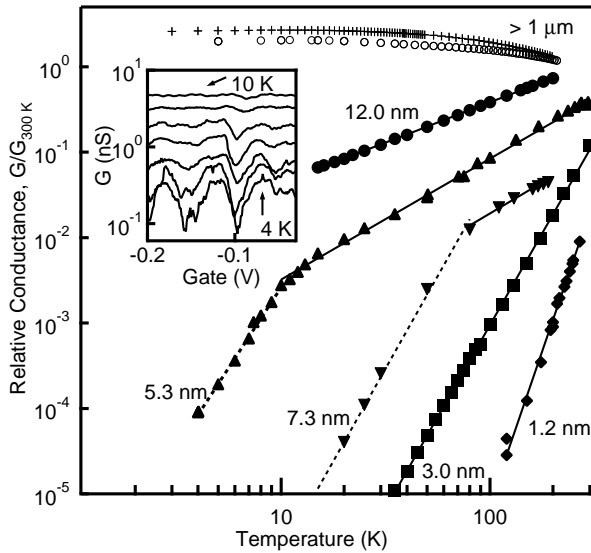


FIG. 2: Relative conductance (G/G_{300K}) versus T for six mesoscopic and two bulk MoSe wires labelled with the wire diameter. Curves are offset vertically for clarity. The solid lines are power-law fits to the data ($G \sim T^\alpha$). The dashed line indicates the region where Coulomb blockade becomes important in two wires (\blacktriangle and \blacktriangledown). Inset: Gate dependence of conductance (G) for the 5.3 nm wire (\blacktriangle) from 4 K to 10 K at 1 K intervals.

conductance decrease with decreasing temperature in the measured temperature range, unlike the samples in the bulk limit ($D > 1 \mu\text{m}$, $L \sim 100 \mu\text{m}$), which exhibit a bulk metallic behavior, as the conductance increases with decreasing temperature, i.e. energy. A power-law dependence, $G \sim T^\alpha$, is evident in these mesoscopic samples, where the exponent α can be readily extracted from the slope of the least-squares fit line in the double logarithm plot. For most of the samples, $G(T)$ can be expressed by a single α within the experimentally accessible conductance range [21]. However, for some wires with a relatively high conductance ($> 1 \mu\text{S}$) at room temperature (Fig. 2 \blacktriangle and \blacktriangledown), an abrupt change in the exponent at low temperatures was observed. In this low temperature regime, the conductance varied with the gate voltage (Fig. 2 inset) and the exponent depended on the applied gate voltage, V_g , due to Coulomb charging effects. Above this Coulomb charging temperature, a general trend of decreasing α with increasing D is found for all mesoscopic samples studied. This trend will be discussed further later in the paper.

We now consider several possible explanations for seeing a decreasing conductance with decreasing temperature. For example, one expects $\ln(G) \propto -1/T$ for barrier activated transport. For highly defective wires, one expects $\ln(G) \propto -1/T^\delta$ due to variable range hopping between localized states in the wire, where δ can range from 1/4 for a 3D wire to 1/2 for a 1D wire [14]. However, neither of these models fit our data as, for all mesoscopic scale measured irrespective of wire diameter, the conduc-

tance follows a power-law remarkably well. Another potential explanation is a non-metallic behavior associated with a Peierls transition, which opens up an energy gap at the Fermi level. However, from the conduction measurements on the bulk quasi-1D crystals ($D > 1 \mu\text{m}$) and also from previous scanning tunneling microscopy work on similar nanowires [12], we observe no evidence for a gap opening at temperatures down to 5 K, consistent with band calculations [15]. Alternatively, a power law dependent tunneling conductance is predicted for tunneling into a Luttinger Liquid, for 1D Wigner Crystals [16], for a highly disordered systems where the electron mean free path is comparable with the wire diameter [17]. We can rule out a 1D Wigner Crystal model since the Coulomb interactions, which are screened by the back gate, are not long-ranged. We also eliminate the scenario for a strongly disordered system by estimating the electron mean free path, l_e in the nanowire. We can estimate l_e indirectly from the effective wire length, L_{eff} , obtained from the dependence of the Coulomb charging energy on the gate voltage. Here, the charging energy $E_c = e^2/C$, where the wire capacitance $C \approx 2\pi\epsilon L_{\text{eff}}/\ln(4L_{\text{ox}}/D)$. For the nanowire device shown in the inset of Fig. 2, the estimated charging energy E_c is 5-10 meV from the conductance map in V and V_g (not shown), from which we obtained $L_{\text{eff}} \sim 0.3 - 0.6 \mu\text{m}$. With this estimate, we rule out the possibility of having a highly disordered system. Moreover, the fact that the measured resistance is larger than $\sim 100 \text{ k}\Omega$ and is not directly correlated with the wire diameter indicates that transport is dominated by tunnelling. Thus a model concerning tunnelling into a relatively clean LL is a more likely description of the observed transport phenomena [22].

Further support for the LL-like transport in the MoSe nanowires can be found in the bias dependence of the conductance in the non-linear response regime. According to the LL model in a tunneling regime [1], the bias voltage dependent transport current, $I(V)$, has a transition between an Ohmic behavior, i.e. $I \propto V$ in the low bias regime ($V \ll k_B T/e$), and a power law behavior with an exponent β , i.e., $I \propto V^{\beta+1}$ in the high bias regime ($V \gg k_B T/e$). The inset of Fig. 3 shows typical $I(V)$ data measured in a mesoscopic wire with the applied bias voltage ranging over more than three orders of magnitude at different temperatures. A transition between Ohmic and power-law behavior is observed as V increases.

Interestingly, we also found that the exponent β depended strongly on D , as can be seen in Table I, where we list α , β and D for 13 samples. In general, we find that α decreases monotonically as D increases. Based on the relation between α and β , we can categorize our samples into two distinct groups: group (I) where $\alpha \approx 2\beta$; and group (II) where $\alpha \approx \beta$. In our experiments, the majority of samples (10 out of 13 in Table I) belongs to group (I), while only a few samples (3 out of 13 in Table I) belong

TABLE I: Measured exponents α and β determined from the temperature and bias dependent conductance measurement, along with the wire diameter (D) as determined by AFM and the number of channels including spin (N) calculated from D . Wires indicated by asterisk (*) have $\alpha \approx \beta$ but for all other wires, $\alpha \simeq 2\beta$.

| Wire | W1 | W2* | W3 | W4 | W5 | W6 | W7 | W8* | W9 | W10 | W11 | W12* | W13 |
|----------|---------------|---------------|---------------|---------------|---------------|---------------|---------------|---------------|---------------|---------------|----------------|----------------|----------------|
| α | 6.6 | 5.2 | 4.3 | 3.95 | 2.33 | 1.40 | 2.34 | 1.1 | 1.55 | 1.95 | 1.2 | 0.94 | 0.61 |
| β | 3.0 | 4.9 | 2.1 | 1.9 | 1.0 | 0.72 | 1.2 | 1.0 | 0.8 | 1.09 | 0.6 | 0.90 | 0.32 |
| D | 0.8 ± 0.5 | 2.1 ± 0.3 | 3.0 ± 0.3 | 3.5 ± 0.2 | 5.0 ± 0.5 | 5.3 ± 1.0 | 6.1 ± 0.5 | 7.2 ± 0.5 | 7.3 ± 1.4 | 7.4 ± 1.5 | 10.3 ± 0.4 | 12.0 ± 0.7 | 15.7 ± 1.1 |
| N | 2 | 12 | 22 | 30 | 62 | 70 | 94 | 130 | 134 | 138 | 268 | 362 | 620 |

to group (II) [23].

For a clean LL without defects, these two exponents are expected to be identical, i.e., $\alpha = \beta$ [1], since they are characteristic of a single junction between FL and LL. The deviation from this model found in group (I) samples can be explained within the LL model with a few defects as described below. Strong defects in the nanowires break the conducting channels into a few LL dots connected in series between the electrodes. In this multiple LL dot scheme, the wires have two kinds of tunnel junctions; (i) junctions between the electrode and wire, constituting a FL to the end of LL junction; and (ii) junctions between two wire segments, constituting an LL to LL junction. In such a wire, the tunneling probability can be specified by two distinct exponents α_{LL-LL} and α_{FL-LL} , where $\alpha_{LL-LL} = 2\alpha_{FL-LL}$ holds [3]. If the linear response resistances of the FL-LL and LL-LL junctions at room temperature are of similar orders of magnitude, we expect $G \propto T^{\alpha_{LL-LL}}$ in the low temperature limit, since the LL-LL junctions become most resistive. However, in the

high bias limit the FL-LL junctions become more resistive than the LL-LL junctions since $\alpha_{LL-LL} > \alpha_{FL-LL}$, and thus $I \propto V^{\alpha_{FL-LL}+1}$. Therefore the exponents obtained from temperature and bias dependent data are expected to have a relation $\alpha = 2\beta$ for wires with a few defects that break them into multiple LL dots, as observed in our group (I) samples [24]. This argument does not hold however if there are no defects in the wire or in the extreme of strong defects that dominate transport within the experimentally accessible range of T and V . For such samples, $\alpha \approx \beta$, which is the relation we find in group (II) samples.

The power-law behaviors in T and V allow us to scale $I(V, T)$ into a single curve [3, 18]. Considering the above arguments, we can modify the scaling formula of a clean LL transport model to include the two exponents α and β as:

$$I = I_0 T^{\alpha+1} \sinh \left(\frac{\gamma eV}{2k_B T} \right) \left| \Gamma \left(1 + \frac{\beta}{2} + i \frac{\gamma eV}{2k_B T} \right) \right|^2 \quad (1)$$

where I_0 and γ are constants independent of T and V . Physically, γ represent the ratio between the voltage across a dominantly resistive junction at high bias to the applied bias voltage [3]. As shown in Fig. 3, the series of $I(V)$ curves measured at different temperatures for the same sample collapse remarkably well onto a single curve described by Eq. 1 over the entire measured temperature range by plotting $I/T^{\alpha+1}$ against $\gamma eV/k_B T$ with only one fitting parameter γ . For the data in Fig. 3, γ is 0.25 ± 0.1 , implying that there are probably four barriers of approximately equal resistance over which the applied bias voltage is distributed.

Finally, we now discuss the dependence of the exponents on the wire diameter (D) in order to elucidate the transition from a few channel 1D transport to the 3D transport limit. For this purpose, we focus on the samples with $\alpha = \alpha_{LL-LL}$ (i.e. group (I) samples and the group (II) samples with $\gamma \approx 1$). In Fig. 4, we show the measured α plotted against D . Since $N \propto D^2$, where N is the number of channels in the wire including the spin degree of freedom [25], the observed rapid decrease of α for large diameter nanowire bundles indicates a cross over from 1D behavior to 3D transport ($\alpha \approx 0$). Employing the electron-electron interaction parameter for a single chain ($N=2$), g , the end tunneling exponent α_{LL-LL} for

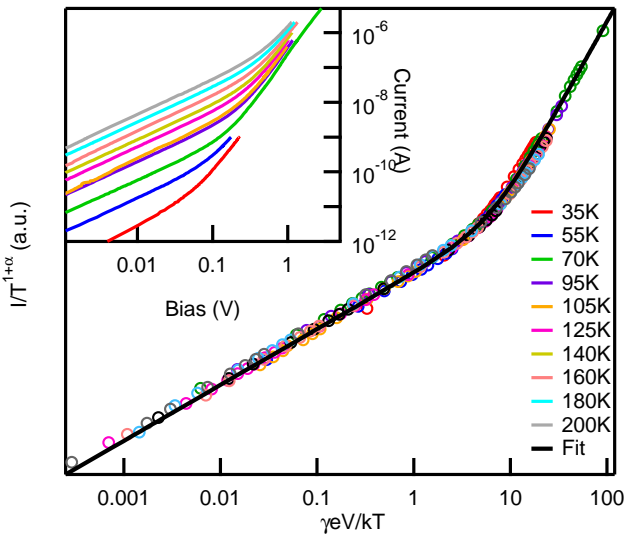


FIG. 3: (color) Inset: Wire W3 I-V data taken at different temperatures between 35 K and 200 K. All curves show a change from linear response to power-law dependence at a temperature dependent bias voltage. Main panel: $I/T^{\alpha+1}$ determined from I-V data plotted against $\gamma eV/k_B T$ with Eq. 1 fit to the data. The measured exponents are $\alpha = 4.3$ and $\beta = 2.1$ ($\sim \alpha/2$) and the fitting parameter γ is 0.25 ± 0.1 .

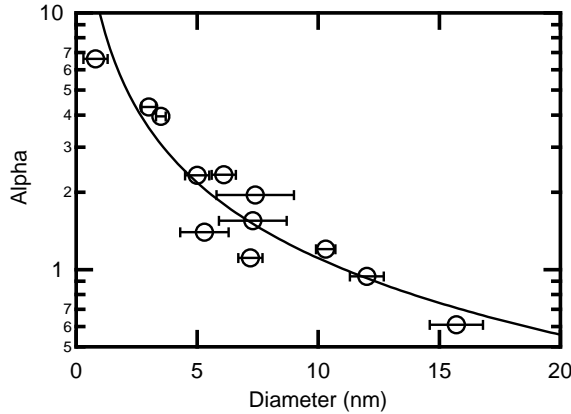


FIG. 4: The exponent α , plotted against the wire diameter D . The solid line is a fit to Eq. 2.

an N channel LL wire can be expressed as [8, 19]:

$$\alpha_{LL-LL} = \frac{2}{N} \left[(1 + NU)^{1/2} - 1 \right], \quad (2)$$

where $U \simeq 2/g^2$. We fit this equation to our data using g as a single fitting parameter. A good agreement with the experimental observation was obtained for $g = 0.15$. For a screened Coulomb interaction, g can be estimated by $g \simeq \sqrt{1/(e^2 \ln(4L_{ox}/a_0) / \pi \hbar v_F \kappa)}$ [8], where v_F is the Fermi velocity of a single chain and κ is the dielectric constant of silicon dioxide. From the fit in Fig. 4, we deduce that $v_F = 3 \times 10^4$ m/s. We note here that this value is smaller than the value obtained from recent band calculation (4×10^5 m/s) [15], indicating that a static screening picture considered in this model might be too simplistic. Further theoretical considerations including the effect of impurities and inter-chain hopping are needed to elucidate strongly interacting electrons in these 1D channels.

We thank C. M. Lieber, Y. Oreg, A. Millis, I. Aleiner, B. Altshuler and R. Egger useful discussions. This work was supported by NSF Award Number CHE-0117752, by the New York State Office of Science, Technology, and Academic Research (NYSTAR). This work used the shared experimental facilities supported by MRSEC Program of the NSF (DMR-02-13574). Y.S.H acknowledges support from the Korean Science and Engineering Foundation. P.K. acknowledges support from NSF CAREER (DMR-0349232) and DARPA (N00014-04-1-0591).

- [4] Z. Yao, H. Postma, L. Balents, and C. Dekker, *Nature (London)* **402**, 273 (1999).
- [5] A. Bachtold, M. de Jonge, K. Grove-Rasmussen, P. McEuen, M. Buitelaar, and C. Schönenberger, *Phys. Rev. Lett.* **87**, 166801 (2001).
- [6] E. Slot, M. Holst, H. van der Zant, and S. Zaitsev-Zotov, *Phys. Rev. Lett.* **93**, 176602 (2004).
- [7] A. N. Aleshin, H. Lee, Y. Park, and K. Akagi, *Phys. Rev. Lett.* **93**, 196601 (2004).
- [8] K. Matveev and L. Glazman, *Phys. Rev. Lett.* **70**, 990 (1993).
- [9] N. Sandler and D. Maslov, *Phys. Rev. B* **55**, 13808 (1997).
- [10] J. M. Tarascon, F. DiSalvo, C. Chen, P. Carroll, M. Walsh, and L. Rupp, *J. Solid State Chem.* **58**, 290 (1985).
- [11] J. Golden, F. DiSalvo, J. Fréchet, J. Silcox, M. Thomas, and J. Elman, *Science* **273**, 782 (1996).
- [12] L. Venkataraman and C. Lieber, *Phys. Rev. Lett.* **83**, 5334 (1999).
- [13] J. Tarascon, G. Hull, and F. DiSalvo, *Mat. Res. Bull.* **19**, 915 (1984).
- [14] Y. Imry, *Introduction to Mesoscopic Physics* (Oxford University Press, New York, 1997).
- [15] F. Ribeiro, D. Roundy, and M. Cohen, *Phys. Rev. B* **65**, 153401 (2002).
- [16] H. Maurey and T. Giamarchi, *Phys. Rev. B* **51**, 10833 (1995).
- [17] R. Egger and S. Gogolin, *Phys. Rev. Lett.* **87**, 066401 (2001).
- [18] L. Balents, cond-mat/9906032.
- [19] R. Egger, *Phys. Rev. Lett.* **83**, 5547 (1999).
- [20] The mesoscopic wires were susceptible to structural deformations locally at the wire/electrode junctions. Due to the invasiveness of the electrodes, multi-terminal measurements were not possible.
- [21] Since G decreases rapidly as T decreases in the nanowire samples, most of our $G(T)$ data were limited at low T by our current sensitivity (10^{-13} A).
- [22] We note that the environmental Coulomb blockade (ECB) model (see for example, Ingold and Nazarov, cond-mat/0508728) might be applied to our experiment. However, its validity is limited to the large N limit [8], where the LL and ECB models do not offer any observable differences in our experimental setup and we thus consider only the LL model in this paper.
- [23] Group (II) samples can be sub-divided further into a group with notable defects such as the one shown in Fig. 1(b) ($\gamma \approx 1$) and a group without strong defects ($\gamma \approx 1/2$), where the parameter γ is defined in Eq. 1.
- [24] For temperatures below 300 K, the deviation of the measured α from α_{LL-LL} is less than 10% as long as $R_{Lead-Wire}/R_{Defect}$ is between $\sim 0.1 - 10$ where $R_{Lead-Wire}$ is the total resistance between the wire and the Au lead and R_{Defect} is the total resistance of all defects. A similar tolerance range for $R_{Lead-Wire}/R_{Defect}$ is also found for $\beta \approx \alpha_{FL-LL}$. We have observed a few devices outside of this tolerance limit, which shows an intermediate bias ranges where LL-LL tunnelling is dominant at low temperature.
- [25] We use $N = 2fD^2/a_0^2$ where f , the filling factor, is 0.91 assuming a hexagonal close packing of the chains.

- [1] J. Voit, *Rep. Prog. Phys.* **57**, 977 (1994).
- [2] A. Chang, L. Pfeiffer, and K. West, *Phys. Rev. Lett.* **77**, 2538 (1996).
- [3] M. Bockrath, D. H. Cobden, J. Lu, A. G. Rinzler, R. E. Smalley, L. Balents, and P. L. McEuen, *Nature (London)* **397**, 598 (1999).